Evaluation of pigtail macaques as a model for the effects of copper intrauterine devices (IUDs) on HIV infection

Robyn M. Engel[1], **Monica Morris**[2], **Tara Henning**[3], **Jana M. Ritter**[4], **Tara L. Jones**[4], **Sharon Dietz**[1], **Jessica Ayers**[1], **Sundaram A. Vishwanathan**[3], **Leecresia Jenkins**[3], **Sherif Zaki**[4], **Dirk Wildemeersch**[5], **David Garber**[3], **Nathaniel Powell**[1], **R. Michael Hendry**[3], **Janet McNicholl**[3], and **Ellen N. Kersh**[3],*

[1]Animal Resources Branch, Division of Scientific Resources, National Center for Emerging and Zoonotic Infectious Diseases, CDC, Atlanta, GA

[2]Total Solutions, Atlanta, GA

[3]Laboratory Branch, Division of HIV/AIDS Prevention, National Center for HIV/AIDS, Viral Hepatitis, Sexually Transmitted Disease, and Tuberculosis Prevention, CDC, Atlanta, GA

[4]Infectious Diseases Pathology Branch, Division of High Consequence Pathogens and Pathology, National Center for Emerging and Zoonotic Infectious Diseases, CDC, Atlanta, GA

[5]Contrel, Gynecological Outpatient Clinic and IUD Training Center, Ghent, Belgium

Abstract

Background—Long-acting, hormonal contraception may increase HIV risk. Copper intrauterine devices (IUDs) could serve as non-hormonal alternatives. We pilot a pigtail macaque model for evaluating HIV susceptibility factors during copper IUD use.

Methods—Frameless and flexible GyneFix® copper IUDs were surgically implanted into three SHIV$_{SF162p3}$-positive macaques via hysterotomy and monitored for up to four months. Four macaques served as no-IUD controls.

Results—All animals retained the devices without complications. No consistent change in vaginal viral RNA or inflammatory cytokines was seen. Two animals had altered menstrual cycles and experienced marked thinning of vaginal epithelium after IUD insertion. Histological examination of uterine tissue at necropsy revealed endometrial ulceration and lymphocytic inflammation with glandular loss at sites of direct IUD contact.

Conclusions—Although the need for insertion surgery could limit its usefulness, this model will allow studies on copper IUDs and SHIV shedding, disease progression, and HIV susceptibility factors.

*Corresponding author: Ellen Kersh, 1600 Clifton Rd NE MS A25, Atlanta, GA 30333; phone (404) 639-2728; fax (404) 639-4278, ekersh@cdc.gov.

Keywords

contraception; SHIV; susceptibility; transmission risk; non-human primate

Introduction

There is ongoing debate regarding the effect of the long-acting, progestin-only, injectable hormonal contraceptive Depot medroxyprogesterone acetate (DMPA) on HIV acquisition risk in women (reviewed in [1]). In 2012, the WHO convened a technical consultation to review evidence regarding hormonal contraception and HIV acquisition [2]. The panel concluded the data were not sufficient to discourage women at risk for HIV from using injectable hormonal contraception, and recommended an "expansion of contraceptive method mix and further research on the relationship between hormonal contraception and HIV infection" [2]. The copper-releasing intrauterine device (CuIUD) has been suggested as a safe alternative to hormonal contraception. CuIUDs are long-acting, reversible, and highly effective in preventing pregnancy. Only a few studies on the relationship between CuIUDs and HIV acquisition risk have been done (reviewed in [3]), in part because CuIUD use is rare in geographic areas of high HIV burden. The limited data available do not suggest an association with increased HIV risk [3]. To allow further studies on the issue, we here introduce a CuIUD animal model. This model is being developed with the goal of conducting comparative studies of the effects of different contraceptive methods on mucosal/ vaginal HIV acquisition, including analysis of biological susceptibility factors in genital tissues.

In women, CuIUDs do not cause obvious extrauterine effects or suppress ovulation. Released copper ions are thought to alter endometrial architecture, the metabolism of endometrial cells, and characteristics of cervical mucus and endometrial secretions (reviewed in [4]). It is also well-documented that CuIUDs evoke an inflammatory response in the uterus of women [4–6]. It has been proposed this inflammation exerts the CuIUD's contraceptive effect, because it is toxic to sperm and ova and impairs fertilization and implantation [5]. There is no evidence to suggest these IUD-induced inflammatory processes affect HIV acquisition or transmission risk [3, 7]. However, reproductive tract inflammation is thought to be a risk factor for HIV acquisition [8]. Sexually transmitted infections can increase female susceptibility to HIV infection [9, 10], likely by recruiting target cells to the genital mucosa. If CuIUDs also recruit target cells to the reproductive tract, they may in turn increase risk of HIV acquisition and transmission. On the other hand, copper ions have been shown to have an anti-viral effect *ex vivo* [11], and this could protect the CuIUD user from HIV infection. A non-human primate model to further investigate these issues would be useful.

IUDs were thoroughly researched in non-human primates, most notably rhesus macaques, in the 1960s in preparation for human use [4, 5]. The research was summarized in a 1968 presentation to the FDA [4]. These studies, which focused on the reproductive effects of IUDs, preceded the era of HIV/AIDS. There are more recent examples of IUD studies in macaques, but there are no available animal model data concerning the effect CuIUDs may

have on HIV. Our efforts in designing this animal model focused on size and shape selection of the IUD, and on evaluating HIV susceptibility parameters such as inflammation and vaginal thinning. We selected pigtail macaques for our studies because of their previous use in HIV prevention research. To our knowledge, the species has only been used once to study hormone-delivering IUDs [12]. Pigtail macaques have year-round lunar menstrual cycles similar to women. We saw this as an advantage to rhesus macaques, which breed and cycle seasonally. Further, pigtail macaques are larger than cynomolgus macaques, another species suitable for HIV research. Larger body and uterine size made it possible to find an appropriate CuIUD, which was similar to those used in women. The main drawback of this model is the sigmoidal, tortuous shape of the cervical lumen [12, 13]. This makes cervical IUD insertion challenging, and there are no published studies describing a cervical approach. Rather, IUDs are traditionally inserted into macaques surgically via laparotomy followed by hysterotomy [12].

We hypothesized CuIUDs would be well tolerated by pigtail macaques. Further, we hypothesized the CuIUDs would cause a local inflammatory response in the uterus, with unknown effects on genital HIV shedding and HIV susceptibility factors such as cervico-vaginal inflammation, epithelial thickness, and vaginal pH.

Materials and Methods

Humane Care Guidelines

Four adult female pigtail macaques (*Macaca nemestrina*) were housed at the Centers for Disease Control and Prevention (CDC) in individual enrichment cages. Animals were housed and cared for according to the recommendations in the *Guide for the Care and Use of Laboratory Animals* [14]. All experiments performed were approved by the Institutional Animal Care and Use Committee (IACUC) of the CDC and were performed according to the guidelines for laboratory animal care and use set forth by the National Institutes of Health (NIH). All animals were $SHIV_{SF162P3}$-positive at the beginning of the study. We used SHIV-positive animals, because they were readily available from other HIV acquisition studies in our group. 2.5432 (seven years old, infected six months, hereafter referred to as IUD1), BB1247 (five years old, infected six months, hereafter IUD2), and Pvi2 (seven years old, infected five months, hereafter IUD3) underwent IUD implantation surgery. CV85 (13 years old, infected 18 months, hereafter C1) was used as a non-surgical control. Animals were anesthetized with 10mg/kg intramuscular ketamine prior to sampling procedures. The only exception to this was when vaginal biopsies or surgery was performed, at which time 3mg/kg intramuscular Telazol was used as an anesthetic. At the conclusion of the study, all animals were humanely euthanized with intravenous pentobarbital (>100mg/kg). Uterine tissue from three additional $SHIV_{SF162P3}$-positive pigtails was collected at necropsy for use as histology controls. These animals, Prf2 (eight years old), Pok2 (six years old) and Pnh2 (seven years old), had been enrolled in an unrelated HIV study. They were sacrificed close to day one of their menstrual cycles, approximately four months after SHIV infection. These animals are referred to as C2, C3 and C4 respectively.

Menstrual Cycle Observations and Progesterone Analysis

Cycle day was determined using a combination of physical observations (sex swelling and visible menstrual bleeding) and plasma progesterone analysis. Throughout the study, animals were observed in their enclosures every other day to look for menstrual blood and to monitor swelling of the perineal sex skin. Swelling was rated on a scale of one to four, with one being the least swollen and four being the most swollen. The animals were anesthetized weekly and a pelvic exam was performed using a pediatric speculum and colposcope. To verify physical observations of the menstrual cycle, plasma was collected weekly from the femoral vein in Vacutainer tubes (CPT: BD, Franklin Lakes, NJ, USA) and progesterone content determined by EIA (Wisconsin National Primate Center).

SHIV RNA Analysis

SHIV RNA was extracted from 1ml aliquots of plasma using the NucliSens system (BioMerieux, Durham NC), according to the manufacturer's protocol. RNA levels were quantified using an internally controlled and normalized reverse-transcription real-time TaqMan© PCR (Applied Biosystems, Carlsbad, CA, USA) assay with a threshold sensitivity level of 50 copies per milliliter [15]. One polyester swab was used to collect secretions from the vaginal vault of each animal for viral load analysis. These swabs were immediately placed in RNA*later* (Applied Biosystems, Carlsbad, CA, USA) and processed as previously described [16].

Mucosal Cytokine Analysis and Vaginal pH

Merocel ophthalmic sponges (Medtronic, Jacksonville, FL, USA) were used to collect vaginal secretions for cytokine analysis. The sponge was placed in the vaginal vault and allowed to sit for at least two minutes prior to removal. Sponges were processed using a protocol and buffer as described [17]. GM-CSF, IL-6, IL-1beta and IL-1R-antagonist (IL-1Ra) levels were measured with Luminex technology using a non-human primate bead kit from Millipore (MPXPRCYTO, Billerica, MA), and normalized to secretion weight. Vaginal pH was also monitored weekly using test strips. Samples collected during menstruation and some post-operative time points were excluded due to blood contamination.

Surgical Description and Follow-Up Monitoring

After injectable anesthesia, animals were intubated and maintained with isoflurane gas at 1–3%. Standard sterile surgical techniques were used. A laparotomy was performed by making a ventral midline incision into the peritoneal cavity, approximately 3cm cranial to the pubic symphysis. A stab incision was made through the apical uterine fundus to gain access to the uterine lumen. Minor persistent hemorrhage at the uterine incision site during the procedure was controlled with manual pressure. 3–0 Ethilon was used to make a single, deep bite into the myometrium from the luminal surface. Cylinders from the frameless and flexible copper-releasing intrauterine device (GyneFix® Contrel Research, Ghent, Belgium) were threaded onto the suture and tied. To accommodate the small uterine size in this species, only two copper cylinders were inserted. The IUD was then gently tucked into the uterine lumen. The uterine wall was closed using 3–0 PDS in a Cushing pattern. The abdominal wall was closed

in three layers. The animals were extubated when the swallowing reflex was apparent. Animals were given Meloxicam 0.2 mg/kg PO the afternoon before surgery and continued on 0.1 mg/kg PO daily for seven days post-operatively. Animals were also administered Buprenorphine Sustained Release 0.2 mg/kg SQ the morning of surgery. For the first 10 days post-operatively the animals were observed daily in their enclosures for bleeding and any signs of pain or distress. After the first 10 days, animals were sedated and examined weekly. This weekly exam included a visual pelvic exam as well as palpation of the uterus. Abdominal radiographs were taken monthly to ensure the IUD remained in place.

Tissue Collection, Histology, and Immunohistochemistry

Prior to IUD placement, vaginal biopsies were collected on the following cycle days during the luteal and follicular phases (C1 days 7 and 21, IUD1 days 7 and 21, IUD2 days 14 and 28, IUD3 days 5 and 19). At each sampling, three pinch biopsies were collected per animal using a rigid biopsy punch (EuroMed®). The biopsy samples were fixed in 10% neutral buffered formalin for 72 hours, then processed for routine paraffin histology, sectioned at a thickness of four microns, and stained with hematoxylin-eosin (H&E). Tissues were evaluated by immunohistochemistry to characterize the relative type and number of inflammatory cells present. Primary mouse monoclonal antibodies used and corresponding catalog numbers are as follows: CD3 (M7254, Dakocytomation, Denmark), CD4 (NCL-CD4-1F6, Leica Microsystems, UK), CD8 (RTU-CD8-295, Leica Microsystems, UK), CD68 (M0814, Dakocytomation, Denmark), CD79a (sc-20064, Santa Cruz Biotechnology, Dallas, TX, USA). IHC assays were performed using a polymer-based indirect immunoalkaline phosphatase detection system with colorimetric detection of antibody/polymer complex with Fast Red Chromogen. All reagents were from Thermo Fisher Scientific (Runcom, Cheshire, UK) unless otherwise specified. Four micron sections of formalin-fixed paraffin embedded tissue were deparaffinized and rehydrated using gradations (100%, 95%, and 70%) of ethanol. Pretreatment with Antigen Retrieval (Biocare Medical, USA) using Biocare's Decloaking Chamber for 30 seconds at 125° C or Proteinase K (Roche, Mannheim,Germany) digestion for 15 minutes at room temperature (RT) was performed, after which Ultra V Block was applied for 10 minutes at RT. Tissues were then incubated with the primary antibody (30 minutes at RT), followed by Primary Antibody Enhancer (10 minutes at RT), AP Polymer (15 minutes at RT), and Naphthol Phosphate Substrate/Fast Red Tablet (20 minutes at RT). Sections were counterstained in Mayer's Modified Hematoxylin (Poly Scientific, Bayshore, NY, USA). Appropriate positive and negative controls were run in parallel. Pigtail macaque lymph node and splenic tissues were used as positive controls. For negative controls, the primary antibodies were replaced with normal mouse sera (CDC).

At necropsy the reproductive tract was removed. The tissue was rinsed with sterile saline, placed on a sterile drape and cut in sagittal section just off midline. After IUD removal, the reproductive tract was placed in 10% neutral buffered formalin for five to seven days. Transverse sections of uterus (one section in contact with the IUD and one section not in contact with the device) and vagina were later processed for routine paraffin histology, sectioned at a thickness of four microns, and stained with H&E. Tissues were also analyzed with immunohistochemistry as described above.

Vaginal epithelial thickness measurement

Vaginal epithelial thickness was measured with AxioVision SE 4.8.3 software (Carl Zeiss, Inc.) on H&E-stained sections using a Zeiss Axioskop microscope interfaced to a digital camera (AxioCam MRc5, Carl Zeiss, Inc.). Measurements were taken at 100 micron intervals along the epithelial basement membrane. Total epithelial thickness was measured from the basement membrane to the epithelial surface, perpendicular to the tangent of the curve of the epithelial surface at that point. Thickness of the keratinized layers was also measured in a similar manner. Thickness of the nucleated cell layer was then calculated by subtraction of keratinized layer thickness from total epithelial thickness. Areas were excluded from analysis if the tissue was highly folded or sectioned tangentially. Twenty-seven to 178 measurements were taken for each tissue section, depending on the quality of the biopsy. One hundred twenty-five to 178 measurements were taken for all sections obtained at necropsy.

Statistical methods

Viral loads, pH, and cytokine values were compared before and after IUD insertion. We built median values for each IUD-bearing animal (IUD1, IUD2, and IUD3) before and after IUD insertion and used paired, two-tailed student's t-tests to compare viral loads, cytokine levels, and pH before and after IUD insertion.

Results

IUD design, insertion and retention

The pigtail macaque uterus is smaller and has a different shape from that of humans. To accommodate this, we selected the frameless, flexible, uni-dimensional copper IUD "GyneFix® 200" or "GyneFix® mini" in use in Europe and Asia [18]. This device, originally designed for women with a small uterus (young, nulliparous, or other conditions), is composed of four copper cylinders threaded onto polypropylene suture. The first and fourth cylinders are crimped to the string so the cylinders cannot slide up and down, and the top end of the device is further secured by a knot. Each cylinder measures 5mm in length and 2.2mm in diameter. We planned to insert the device cervically, as is standard procedure in women, which entails anchoring the knot into the myometrium at controlled depth. However, when we inspected two pigtail macaques not associated with this study at necropsy, we found a sigmoidal, "corkscrew"-like cervical canal as described by others [12, 13]. This was judged a substantial obstacle to safe cervical insertion by the attending veterinarian, and surgical implantation via hysterotomy was performed as a safer alternative.

Three SHIV-positive pigtail macaques in good health (IUD1, IUD2, and IUD3), and without onset of SAIDS, underwent hysterotomy. The animals had been monitored for 8 to 20 weeks to obtain an accurate assessment of menstrual cycling patterns. During surgery, we decided to insert only two of the four cylinders included in the GyneFix® 200 device, due to the small size of the uterine lumen (Fig 1A). All macaques recovered from surgery without complications. One week after surgery, we began to anesthetize animals again to perform physical exams, blood draws, and to obtain x-rays and ultrasounds to monitor the position of the IUD and the condition of the uterus. Figure 1 shows representative ventrodorsal (B) and

lateral (C) radiographs with the device clearly visible. All IUDs were retained for the length of the study, and no animal showed any signs of fluid accumulation in the uterine lumen or abnormal cervical discharge. Further size fitting information was obtained at necropsy when the macaques were humanely euthanized 11, 18, and 19 weeks after surgery. Figure 1D displays the female reproductive tract at necropsy, showing the opened uterus with IUD in place, and sigmoidal cervix and vagina visible to the right. The two copper cylinders filled a substantial part of the uterine lumen. Figure 1E shows the same tissues after the IUD was removed. Shallow indentations in the mucosal surfaces at sites of direct contact with the IUDs are apparent. Indented areas had smooth, glistening surfaces and appeared grossly non-inflamed. Of note, a control animal (C1) without IUD was also enrolled throughout the duration of the study, for 30 weeks. It was withdrawn from active study in week eight due to health reasons (excessive bleeding during blood draws, prolonged menstruation and low platelet counts). At necropsy, in its study week 30, C1 was found to have early stage endometriosis, and was thus not a suitable "normal" control for uterine tissue comparisons to IUD1–3 (data not shown). Its vaginal tissue samples were unaffected by endometriosis, and were included in our comparisons. C2, C3 and C4 all had grossly normal uterine tissue.

IUD effects on virus

At the beginning of the study (pre-IUD), the four SHIV-positive macaques had different levels of genital SHIV shedding, ranging from a median undetectable (IUD3, C1), to 400 (IUD1), and 1.4×10^3 copies/ml of vaginal fluid (IUD2) (Fig 2A, medians determined from four to eight time points for pre-, and also for post-IUD time points per animal). After IUD insertion (post-IUD), median SHIV copy numbers declined in IUD1, increased in IUD2, and remained largely undetectable in IUD3, indicating that the CuIUD did not uniformly increase genital SHIV shedding, as is also the case in women [7]. Figure 2B reports corresponding systemic SHIV levels in blood plasma; they also did not change significantly during the study ($p > 0.05$; paired t-test).

IUD effects on susceptibility factors for HIV infection (menstrual cycling, genital inflammation, and pH)

We monitored menstrual cycling pre- and post-IUD insertion, because associated hormonal fluctuations can affect susceptibility to SHIV [19]. To define the menstrual cycle, we observed sex skin tumescence ("sex skin swelling", depicted as grey bars in Fig 3) which peaks during ovulation, and also measured plasma progesterone which rises after ovulation and drops precipitously immediately prior to menstruation (black lines in Fig 3). IUD1 cycled at the beginning of the study, but stopped cycling after IUD insertion. IUD2 initially kept cycling after surgery, but stopped post-operatively after three progesterone peaks. IUD3 cycled throughout the study (pre- and post-IUD), as did the no-IUD control, C1.

The macaque vaginal epithelium thins during the luteal phase of the menstrual cycle, and also during administration of progestin-based contraceptives [20]. It has been hypothesized that thinned epithelium increases vulnerability to SHIV infection [20]. Although not expected to change with the nonhormonal CuIUD as a contraceptive method, we evaluated this HIV susceptibility factor for future comparison to what is seen with progestin-based contraceptives. We measured thickness of vaginal epithelium pre-operatively, in the

follicular and luteal phases, and compared these measurements to those at necropsy. Figure 4 shows representative vaginal tissues at each time point. As expected, the mucosa consisted of thick nucleated epithelium with keratinization during the follicular phase (Fig 4A, left), and underwent thinning of both nucleated and keratinized layers in the luteal phase (Fig 4A, middle). After IUD implantation, there was marked thinning of the nucleated layer and an absence of keratinization in the two animals that stopped cycling (IUD1 and IUD2) (Fig 4A, right). Thinning was much more pronounced after IUD implantation than thinning during the pre-operative luteal phase. These findings are shown quantitatively in Fig 4B. The mean thickness of the nucleated epithelial layer at necropsy was 71 and 82 microns in IUD1 and IUD2 respectively, while it was 347 and 227 microns in IUD3 and C1, respectively.

We also evaluated vaginal inflammatory infiltrates by immunohistochemistry. The predominant cell type was CD3+ T lymphocytes in tissues from both CuIUD-bearing and control animals (Fig 4C, and data not shown). CD68+ macrophages and unstained granulocytes were present in fewer numbers in all animals (data not shown). CD79a+ B lymphocytes and plasma cells were rarely seen (not shown). T cells were commonly seen at the mucosal-submucosal junction and transmigrating into the mucosa (Fig 4C). In areas where the vaginal epithelium was thicker than 100 microns, the transmigrating T cells were confined to the basilar epithelial layers and rarely reached the luminal surface (Fig 4C, left and middle). In contrast, where the epithelium was very thin, most notably in necropsy tissues from IUD1 and IUD2, transmigrating T cells frequently reached the surface epithelium (Fig 4C, right). T cell infiltrates comprised mostly CD8+ cells, with fewer CD4+ cells (data not shown), the latter being target cells for HIV infection. There was no notable difference in B cell, macrophage, or CD4+ T cell numbers or distribution between phases of the menstrual cycle or after IUD implantation (not shown).

Inflammation and immune activation can affect HIV acquisition, shedding, and disease progression. To further evaluate possible inflammatory processes in the female reproductive tract, either in response to surgery or to the presence of the CuIUD, we measured pro-inflammatory cytokines (GM-CSF, IL-6, IL-1beta, and IL-1R-antagonist) in cervico-vaginal secretions. Mucosal cytokine levels did not change consistently or significantly in our subjects.

Bacterial vaginosis increases risk of HIV infection [21]. The vaginal canal is normally colonized by bacterial microflora that maintain the acidity of this compartment. We measured vaginal pH throughout the study because changes in pH can be indicative of gross changes in the composition of the vaginal microflora. pH rose in each animal after IUD implantation (Fig 5). The median pH pre-IUD was 7.5 compared to 8.7 post IUD (p=0.0378, paired student's t-test, two-tailed).

Uterine histopathology

We examined uterine tissue collected at necropsy to document CuIUD associated changes in tissue architecture and inflammatory cell infiltration. Normal endometrium from a control macaque in the late luteal phase shows epithelial-lined endometrium and a thick stroma with abundant endometrial glands (Fig 6A). Sections of IUD-implanted uterus show endometrial alterations at non-contact and CuIUD contact sites (Fig 6B and C). Areas without direct

CuIUD contact showed variable, segmental epithelial ulceration and glandular loss. When present, ulceration was accompanied by mild superficial stromal lymphocytic infiltrates (Fig 6B). IUD contact areas were associated with more severe ulceration, characterized by endometrial epithelial loss and glandular and stromal attenuation with inflammatory cell infiltration. At points of deepest ulceration, there was full-thickness endometrial loss with only a thin layer of granulation tissue overlying the myometrium (Fig 6C).

We performed immunohistochemistry to characterize the inflammation associated with CuIUDs, which is purportedly linked to their contraceptive function. In all examined uterine tissues of both CuIUD-implanted and control animals, CD3+ T lymphocytes were the most prevalent inflammatory cell type seen, and CD8+ cells were more numerous than CD4+ cells (data not shown). CD68+ macrophages were present in low numbers and scattered throughout all sections (data not shown). CD79a+ B lymphocytes were the least prevalent cell type seen (data not shown). In control uterine tissues, T cells were uniformly scattered individually and in small aggregates throughout the endometrial stroma and around myometrial vessels (Fig 6D). In contrast, in IUD-implanted animals, T cell infiltrates were increased in noncontact areas and even more so in contact areas with discontinuous epithelium (Fig 6E and F). In non-contact areas, T cells were concentrated in the superficial submucosa, mostly near areas of ulceration (Fig 6E). In contact ulcer beds, T cells were most concentrated at the periphery of the lesion and in surrounding superficial endometrial and periglandular stroma (Fig 6F).

Discussion

The goal of this study was to develop a CuIUD macaque model for HIV acquisition, disease progression, and transmission research. We were able to implant a modified GyneFix® CuIUD into SHIV-positive pigtail macaques, making this the first published study to use any IUD in SHIV- or SIV-infected macaques, and the first CuIUD study in pigtail macaques. Several features of human CuIUD use appeared to be modeled accurately in our study. The CuIUDs were generally well tolerated after implantation, and could have remained in place for longer than our pre-defined three month study period. CuIUD implantation caused physical endometrial changes similar to that seen in women [4]. Also consistent with observations in women, the CuIUDs did not significantly change genital SHIV shedding [7]. The model differed from human use in other aspects, however. Foremost, the need to perform implantation surgeries introduced wound healing processes that may increase inflammation and HIV susceptibility. Second, we observed unexpected changes to menstrual cycling in two of three animals after IUD implantation, accompanied by severe thinning of the vaginal mucosa. These findings may limit the usefulness of this model for some aspects of HIV acquisition studies. Nevertheless, the study may also form the basis for future research efforts to refine a pigtail macaque CuIUD model.

One ideal refinement of this model would be cervical insertion of the CuIUD. Cervical insertion of a smaller device than the GyneFix® 200 in combination with osmotic dilators and cervical ripening agents may be possible. Transcervical uterine lavage using equipment modified to accommodate the small size of the FRT has been accomplished in macaques [22]. In addition, the "Chai technique" [23] has been successfully used in baboons to

overcome challenging cervical insertion of IUDs. However, baboons are much larger than macaques and have a straight cervical canal. For these reasons, the success of this technique is uncertain in macaques. If surgeries remain necessary, the impact on HIV risk factors may be lessened by allowing the animals to recover for one month as done here, or even longer.

As a further refinement, we suggest testing an even smaller IUD in future studies. Distension of the uterus by devices can inhibit ovulation or corpus luteum formation in some species (reviewed in [4]). Therefore, it is possible the cessation of menstrual cycles in two of our macaques was due to an oversized device. A smaller device would also help to alleviate some of the pressure-induced endometrial damage seen in our subjects. The simplest solution would be to implant just one GyneFix® cylinder. Other methods to deliver more copper ions with a smaller device include devices that also release silver or nano-particle delivery (Dirk Wildemeersch, personal communication).

We focused on evaluating how a CuIUD affects HIV risk and susceptibility factors. Of these, the observation of excessive vaginal thinning was unexpected. One explanation for this is cessation of menstrual cycling, which is supported because it only occurred in animals that stopped cycling. However, it remains unclear why post-IUD implantation thinning exceeded pre-operative luteal phase thinning even though progesterone levels were low in these animals. Estrogen levels in IUD1 and IUD2 were low, but were comparable to levels in IUD3 and C1 which had no excessive thinning (data not shown). The thinning may also have been caused by the stress of surgery or the study in general, or the presence of the CuIUD. Whatever the cause of the thinned epithelium, its effects on the proximity of inflammatory cells to the vaginal lumen were striking. The predominant cell type found in vaginal tissue was T lymphocytes. In all subjects, these inflammatory cells were found at the submucosal/mucosal interface. Where thick epithelium was present, as for IUD3 and C1, these migrating cells were limited to the basilar epithelium and rarely reached the luminal surface. However, where epithelium was thin, as in IUD1 and IUD2 at necropsy, migrating cells often reached the superficial mucosal layers and vaginal lumen. This proximity of inflammatory cells to the mucosal surface may have implications for HIV acquisition and transmission.

Another unexpected finding in our subjects was a rise in vaginal pH, likely due to changes in the vaginal microflora. In women, a rise in pH is one indicator of bacterial vaginosis (BV), which may be caused by bacterial translocation during IUD insertion. However, it is not possible to extrapolate criteria for BV diagnosis directly from women to macaques, since normal bacterial populations and pH levels differ between species. Alternatively, the bacterial population could have been affected directly by the copper ions released from the CuIUD. In future studies, genetic analysis of bacterial populations or culture of bacteria from the vaginal vault before and after IUD insertion is recommended to document any changes in the bacterial flora.

It is unknown whether uterine inflammation caused by CuIUDs affects susceptibility to HIV. The development of a CuIUD model can potentially help to answer this question. Women using CuIUDs experience an inflammatory reaction composed of variable numbers of polymorphonuclear cells, macrophages and lymphocytes [4–6]. The CuIUD-bearing

pigtail macaques in our study also experienced increased uterine inflammation when compared to controls. The predominant cell types involved were T lymphocytes. Of primary interest in the context of HIV research was the location of these potential target cell populations. In the uterus of CuIUD-bearing animals, inflammatory cells were concentrated at sites of ulceration and in the superficial subepithelial stroma. This concentration of inflammatory cells at or near the luminal surface is a noteworthy finding, as T cells in direct contact with infected semen are likely to affect HIV acquisition.

A substantial study limitation was the small group size of only three CuIUD animals. All animals were SHIV-positive, allowing analysis of the existing infection, but preventing analysis of susceptibility factors in uninfected animals, as would be most relevant for planned HIV acquisition studies. It remains unknown whether the pre-existing SHIV infection increased inflammatory parameters in CuIUD-bearing macaques beyond potential effects in SHIV-negative macaques. In addition, contraceptive effects of the CuIUD were not evaluated. Therefore, it also remains unknown whether the CuIUD would be able to fulfill its primary contraceptive purpose in this species.

In summary, we introduce a novel macaque model for studies with CuIUDs and SHIV infection. Such research has not previously been undertaken in macaques. Although we encountered obstacles to insertion and size fitting, we show that a CuIUD model for HIV research is feasible, and may provide invaluable sample collection and research opportunities not possible in women. The CuIUD increased suspected HIV susceptibility factors (T lymphocyte infiltration in vagina and uterus, rise in pH, thinning of vaginal epithelium) in this pilot study. We conclude that further evaluation of CuIUDs and HIV acquisition factors in larger study groups and SHIV-negative macaques would be of merit. Further applications for this work could be drug delivery testing of drug-laden IUDs for HIV prevention research, as is critical for recent antiviral prevention trials that suffered from poor user adherence [24].

Acknowledgments

References

1. Polis CB, Curtis KM. Use of hormonal contraceptives and HIV acquisition in women: a systematic review of the epidemiological evidence. Lancet Infect Dis. 2013; 13(9):797–808. [PubMed: 23871397]

2. World Health Organization. Hormonal Contraception and HIV: Technical Statement. Geneva: 2012.

3. Morrison CS, Turner AN, Jones LB. Highly effective contraception and acquisition of HIV and other sexually transmitted infections. Best Pract Res Clin Obstet Gynaecol. 2009; 23(2):263–284. [PubMed: 19211309]

4. Corfman PA, Segal SJ. Biologic effects of intrauterine devices. Am J Obstet Gynecol. 1968; 100(3): 448–459. [PubMed: 15782465]

5. Ortiz ME, Croxatto HB. Copper-T intrauterine device and levonorgestrel intrauterine system: biological bases of their mechanism of action. Contraception. 2007; 75(6 Suppl):S16–30. [PubMed: 17531610]

6. Sheppard BL. Endometrial morphological changes in IUD users: a review. Contraception. 1987; 36(1):1–10. [PubMed: 3117492]

7. Richardson BA, Morrison CS, Sekadde-Kigondu C, Sinei SK, Overbaugh J, Panteleeff DD, Weiner DH, Kreiss JK. Effect of intrauterine device use on cervical shedding of HIV-1 DNA. AIDS. 1999; 13(15):2091–2097. [PubMed: 10546862]

8. Keele BF, Estes JD. Barriers to mucosal transmission of immunodeficiency viruses. Blood. 2011; 118(4):839–846. [PubMed: 21555745]

9. Cohen MS. Sexually transmitted diseases enhance HIV transmission: no longer a hypothesis. Lancet. 1998; 351(3 Suppl):5–7. [PubMed: 9652712]

10. Corbett EL, Steketee RW, ter Kuile FO, Latif AS, Kamali A, Hayes RJ. HIV-1/AIDS and the control of other infectious diseases in Africa. Lancet. 2002; 359(9324):2177–2187. [PubMed: 12090997]

11. Sagripanti JL, Lightfoote MM. Cupric and ferric ions inactivate HIV. AIDS Res Hum Retroviruses. 1996; 12(4):333–337. [PubMed: 8906994]

12. Nayak NR, Slayden OD, Mah K, Chwalisz K, Brenner RM. Antiprogestin-releasing intrauterine devices: a novel approach to endometrial contraception. Contraception. 2007; 75(6 Suppl):S104–111. [PubMed: 17531599]

13. Hafez ESE, Jaszczak S. Comparative anatomy and histology of the cervix uteri in non-human primates. Primates. 1972; 13(3):297–316.

14. National Research Council (U.S.). Guide for the Care and Use of Laboratory Animals. 8th ed.. National Academies Press; Washington D.C.: 2011.

15. Subbarao S, Otten RA, Ramos A, Kim C, Jackson E, Monsour M, Adams DR, Bashirian S, Johnson J, Soriano V, Rendon A, Hudgens MG, Butera S, Janssen R, Paxton L, Greenberg AE, Folks TM. Chemoprophylaxis with tenofovir disoproxil fumarate provided partial protection against infection with simian human immunodeficiency virus in macaques given multiple virus challenges. J Infect Dis. 2006; 194(7):904–911. [PubMed: 16960777]

16. Henning TR, Lacour N, Amedee AM. Efficient methodologies for sensitive HIV-1 RNA quantitation from plasma and vaginal secretions. J Clin Virol. 2009; 46(4):309–313. [PubMed: 19783472]

17. Henning T, Fakile Y, Phillips C, Sweeney E, Mitchell J, Patton D, Sturdevant G, Caldwell HD, Secor WE, Papp J, Hendry RM, McNicholl J, Kersh E. Development of a pigtail macaque model of sexually transmitted infection/HIV coinfection using Chlamydia trachomatis, Trichomonas vaginalis, and SHIV(SF162P3). J Med Primatol. 2011; 40(4):214–223. [PubMed: 21781129]

18. Wildemeersch D, Pett A, Jandi S, Hasskamp T, Rowe P, Vrijens M. Precision intrauterine contraception may significantly increase continuation of use: a review of long-term clinical experience with frameless copper-releasing intrauterine contraception devices. Int J Womens Health. 2013; 5:215–225. [PubMed: 23658502]

19. Vishwanathan SA, Guenthner PC, Lin CY, Dobard C, Sharma S, Adams DR, Otten RA, Heneine W, Hendry RM, McNicholl JM, Kersh EN. High susceptibility to repeated, low-dose, vaginal SHIV exposure late in the luteal phase of the menstrual cycle of pigtail macaques. J Acquir Immune Defic Syndr. 2011; 57(4):261–264. [PubMed: 21546848]

20. Marx PA, Spira AI, Gettie A, Dailey PJ, Veazey RS, Lackner AA, Mahoney CJ, Miller CJ, Claypool LE, Ho DD, Alexander NJ. Progesterone implants enhance SIV vaginal transmission and early virus load. Nat Med. 1996; 2(10):1084–1089. [PubMed: 8837605]

21. Atashili J, Poole C, Ndumbe PM, Adimora AA, Smith JS. Bacterial vaginosis and HIV acquisition: a meta-analysis of published studies. AIDS. 2008; 22(12):1493–1501. [PubMed: 18614873]

22. Goodeaux LL, Anzalone CA, Webre MK, Graves KH, Voelkel SA. Nonsurgical technique for flushing the Macaca mulatta uterus. J Med Primatol. 1990; 19(1):59–67. [PubMed: 2338705]

23. Chai D, Cuneo S, Falconer H, Mwenda JM, D'Hooghe T. Olive baboon (Papio anubis anubis) as a model for intrauterine research. J Med Primatol. 2007; 36(6):365–369. [PubMed: 17976041]

24. Baeten J, Celum C. Oral antiretroviral chemoprophylaxis: current status. Current Opinion in HIV and AIDS. 2012; 7(6):514–519. [PubMed: 22964886]
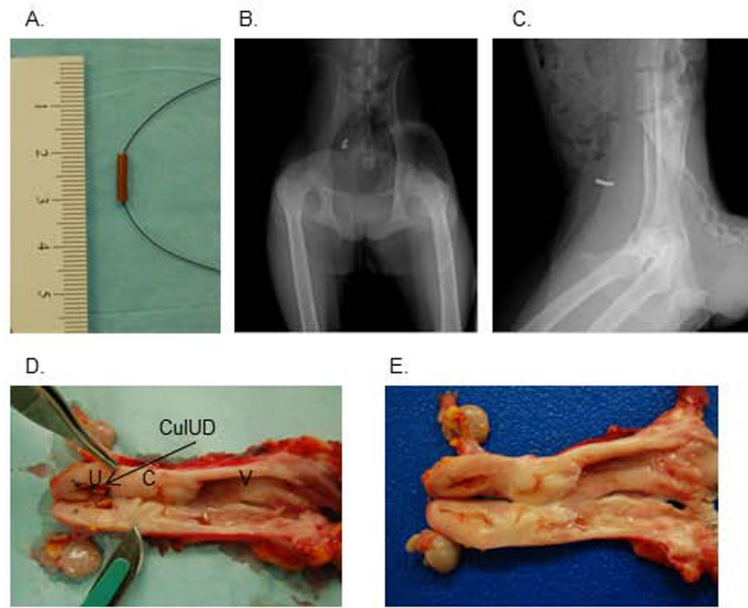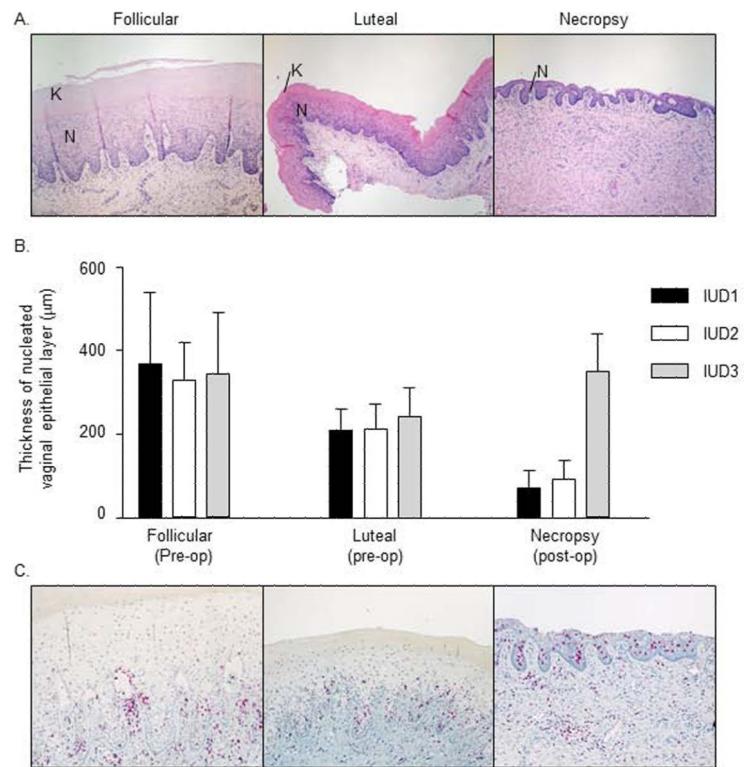
Fig. 1.
Size fit of the CulUD
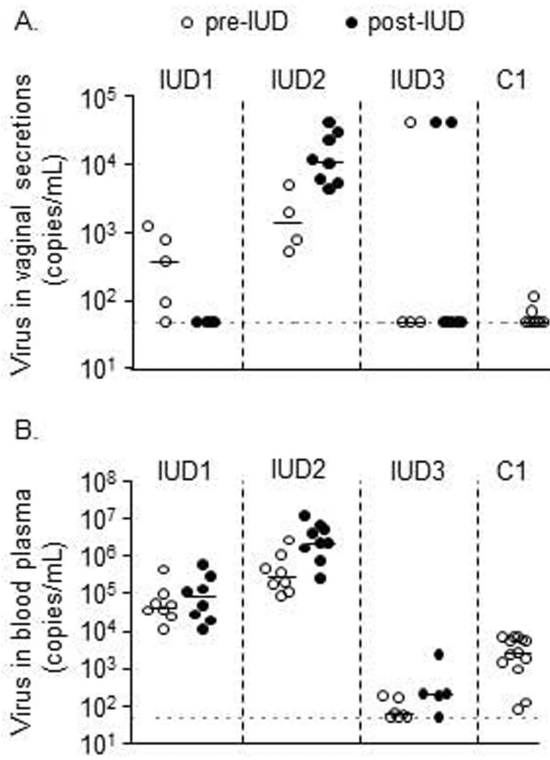
Figure 2.
SHIV$_{SF162P3}$ viral load
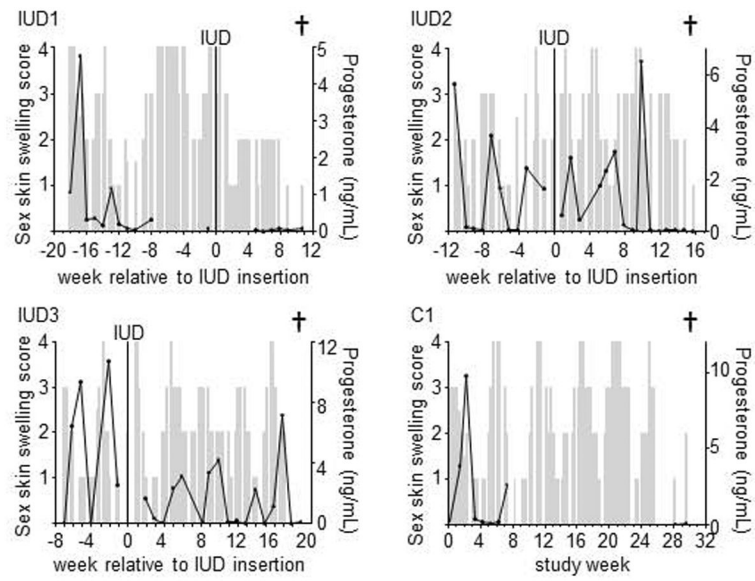
Fig. 3.
Menstrual cycle and CuIUD implantation

Fig. 4.
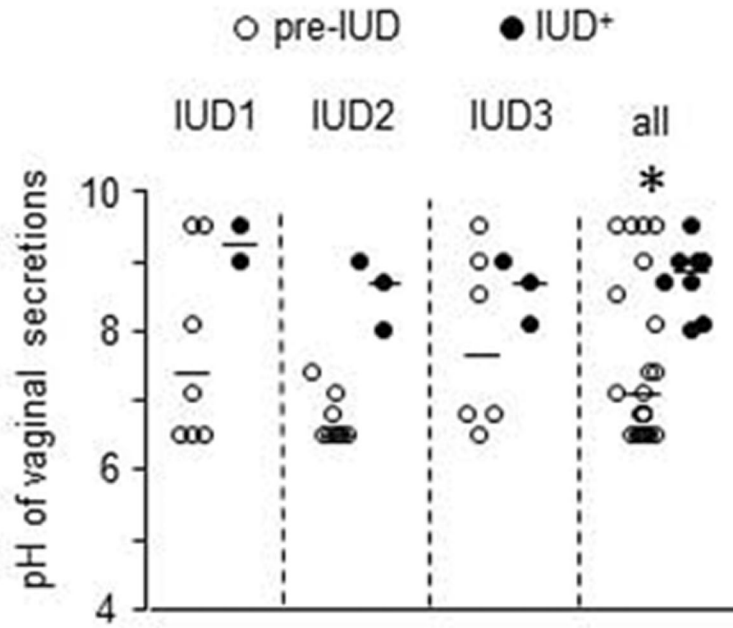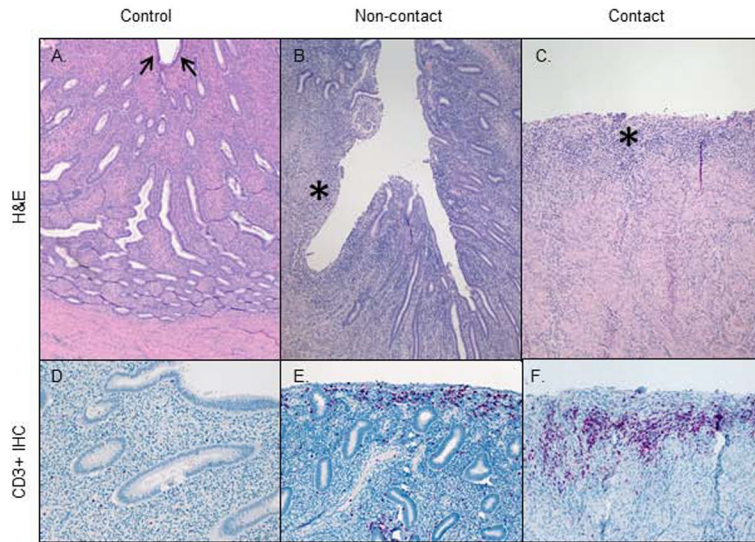Vaginal tissues during CuIUD use

Fig. 5.
CulUD use and vanginal pH

Figure 6.
Uterine pathology at necropsy